Anesthesiology
1999; 91:1733–43

Ketamine Distribution Described by a Recirculatory Pharmacokinetic Model Is Not Stereoselective

Thomas K. Henthorn, M.D., Tom C. Krejcie, M.D.,† Claus U. Niemann, M.D.,‡ Cheri Enders-Klein, B.A.,§ Colin A. Shanks, M.D.,‖† Michael J. Avram, Ph.D.#*

Background: **Differences in the pharmacokinetics of the enantiomers of ketamine have been reported. The authors sought to determine whether these differences extend to pulmonary uptake and peripheral tissue distribution and to test the hypothesis that tissue distribution of the stereoisomers differs because of carrier-mediated drug transport.**

Methods: **The dispositions of markers of intravascular space and blood flow (indocyanine green, ICG) and total body water and tissue perfusion (antipyrine) were determined along with *S*-(+)- and *R*-(−)-ketamine in five mongrel dogs. The dogs were studied while anesthetized with 2.0% halothane. Marker and drug dispositions were described by recirculatory pharmacokinetic models based on frequent early and less-frequent later arterial blood samples. These models characterize pulmonary uptake and the distribution of cardiac output into parallel peripheral circuits.**

Results: **Plasma elimination clearance of the *S*-(+)-ketamine enantiomer, 29.9 ml · min^{-1} · kg^{-1}, was higher than that of the *R*-(−)-enantiomer, 22.2 ml · min^{-1} · kg^{-1}. The apparent pulmonary tissue volumes of the ketamine *S*-(+) and *R*-(−)-enantiomers (0.31 l) did not differ and was approximately twice that of antipyrine (0.16 l). The peripheral tissue distribution volumes and clearances and the total volume of distribution (2.1 l/kg) were the same for both stereoisomers when elimination clearances were modeled from the rapidly equilibrating peripheral compartment.**

Conclusions: **Although the elimination clearance of *S*-(+)-ketamine is 35% greater than that of the *R*-(−)-enantiomer, there is no difference in the apparent pulmonary tissue volume or peripheral tissue distribution between the stereoisomers, suggesting that physicochemical properties of ketamine other than stereoisomerism determine its perfusion-limited tissue distribution. (Key words: Antipyrine; canine; indocyanine green; mean transit time.)**

KETAMINE, a drug used for the induction and maintenance of anesthesia, exists as a racemic (50:50) mixture of *R*-(−)- and *S*-(+)-enantiomers. Previous studies of the pharmacokinetics of ketamine have shown that the disposition of the *R*-(−) and *S*-(+)-enantiomers differ. Studies first showed that the elimination clearance (Cl_E) of the *S*-(+)-isomer exceeded that of *R*-(−) in rodents.[1,2] White *et al.*[3] studied the clinical pharmacology of the two enantiomers of ketamine in humans and found kinetic differences similar to those found previously in animals. A detailed pharmacokinetic study in healthy volunteers by Geisslinger *et al.*[4,5] found differences in both the Cl_E and the volumes of distribution between the two enantiomers. Further investigation showed that there are significant pharmacodynamic differences between the enantiomers as well.[6] The *S*-(+)-enantiomer is approximately twice as potent as a sedative–hypnotic as is the *R*-(−)-enantiomer, whereas the *R*-(−)-enantiomer appears to have a greater potency for producing unwanted psychotropic side effects. These differences in

* Associate Professor of Anesthesiology, Department of Anesthesiology, Northwestern University Medical School. Current position: Associate Professor of Anesthesiology, Department of Anesthesiology, University of Colorado Health Sciences Center, Denver, Colorado.

† Associate Professor of Anesthesiology, Department of Anesthesiology, Northwestern University Medical School.

‡ Research Fellow in Anesthesiology, Department of Anesthesiology, Northwestern University Medical School. Current position: Resident in Anesthesia, Department of Anesthesia, University of California at San Francisco, San Francisco, California.

§ Research Technician in Anesthesiology, Department of Anesthesiology, Northwestern University Medical School. Current position: Graduate Student, University of Illinois at Chicago, College of Pharmacy, Chicago, Illinois.

‖ Professor of Anesthesiology, Department of Anesthesiology, Northwestern University Medical School.

Associate Professor of Anesthesiolgy, Department of Anesthesiology, Northwestern University Medical School.

† Deceased.

Received from the Department of Anesthesiology, Northwestern University Medical School, Chicago, Illinois. Submitted for publication November 10, 1998. Accepted for publication June 22. 1999. Supported in part by the National Institutes of Health (grants GM43776, GM47502, and GM47819), Bethesda, Maryland. Presented in part at the annual meeting of the American Society of Anesthesiologists, New Orleans, Louisiana, October 19–23, 1996.

Address reprint requests to Dr. Henthorn: Department of Anesthesiology, University of Colorado, UCHSC Box B113, 4200 East Ninth Avenue, Denver, Colorado 80262. Address electronic mail to: tkhenthorn@ski.uhcolorado.edu

Table 1. Subject Characteristics and Global Pharmacokinetic Parameters (N = 5)

				ICG		Antipyrine		Ketamine		
	Weight (kg)	Hct (%)	Cardiac Output* (l/min)	V_{SS} (l/kg)	Cl_E (ml · min^{-1} · kg^{-1})	V_{SS} (l/kg)	Cl_E (ml · min^{-1} · kg^{-1})	V_{SS} (l/kg)	$S(+)$ Cl_E (ml · min^{-1} · kg^{-1})	$R(-)$ Cl_E (ml · min^{-1} · kg^{-1})
Mean	30.2	37.6	3.44	0.089	10.14	0.73	2.62	2.11	29.9	22.2
(SD)	(2.4)	(2.4)	(1.82)	(0.005)	(2.80)	(0.08)	(0.49)	(0.72)	(4.5)	(1.7)

Antipyrine and ketamine V_{SS} and Cl_E are here presented on the basis of plasma concentrations.

V_{SS} = the sum of all compartmental volumes (volume of distribution at steady-state); Cl_E = the elimination clearance; Hct = hematocrit.

* Determined by thermal dilution.

pharmacodynamics led to the commercial introduction of the *S*-(+)-enantiomer in the European market.[7]

The intensity and timing of the onset of drug effect for rapidly acting intravenous anesthetics, such as ketamine, are influenced by factors that affect the early arterial drug concentration *versus* time profile.[8] These factors include intravascular mixing, pulmonary uptake, and distribution to highly perfused tissues.[9] Our recently developed recirculatory pharmacokinetic model describes these processes by referencing them to the disposition of markers of intravascular space and body water, indocyanine green (ICG), and antipyrine.[10,11]

It has been suggested recently that distribution of drugs to tissue may be affected by carrier-mediated transport across the endothelium, in addition to blood flow and diffusion.[12] We have shown that pulmonary uptake of fentanyl involves, not only passive diffusion, but also carrier-mediated endothelial transport.[13] Studying the simultaneous disposition of the stereoisomers of ketamine offers a unique opportunity to test the hypothesis that tissue distribution of the stereoisomers differs because of carrier-mediated drug transport because such transport might be expected to be stereoselective. If the distribution clearances of either or both ketamine stereoisomers are affected by carrier-mediated transport, they will differ significantly from that of antipyrine, a pharmacologically inert pharmacokinetic prototype for many lipophilic drugs, including intravenous anesthetics.[14] Antipyrine distributes to a volume as large as total body water,[15] including pulmonary extravascular water,[16] in a blood flow–dependent manner.[17]

Therefore, we sought to study the pulmonary uptake, systemic tissue distribution, and elimination of antipyrine and the *R*-(−) and *S*-(+)-enantiomers of ketamine in dogs using frequent arterial sampling and recirculatory pharmacokinetic analysis.

Materials and Methods

Experimental Protocol

Five male dogs, weighing 27.5–33 kg (30.2 ± 2.4 kg, table 1), were studied in this Institutional Animal Care and Use Committee–approved study. After an overnight fast, during which water was allowed *ad libitum,* the dog was brought to the laboratory. Anesthesia was induced with methohexital (10–15 mg/kg intravenous) *via* a foreleg vein, the trachea was intubated with a 9-mm endotracheal tube, and the animal was placed in the left lateral decubitus position. Mechanical ventilation was instituted at a tidal volume of 20–25 ml/kg and at a rate sufficient to maintain end-tidal carbon dioxide tension at 30 ± 5 mmHg. Anesthesia was maintained with 2.0% halothane in oxygen. End-tidal halothane concentrations were monitored with an infrared multiple gas analyzer (PPG Biomedical Systems, Lenexa, KS) after its calibration with known standards.

Using a modified Seldinger technique, an 8-French percutaneous sheath introducer was inserted into an external jugular vein. Arterial access for blood sampling by roller pump or syringe was achieved by inserting a 16-gauge (Angiocath; Becton Dickinson, Sandy, UT) catheter percutaneously into the femoral artery; this also allowed systemic arterial blood pressure to be monitored *via* a solid-state pressure transducer (Baxter-Edwards, Irvine, CA). A flow-directed thermal dilution pulmonary artery catheter (Baxter-Edwards 93A-140-7F, with a 20-cm proximal port) was inserted through the sheath introducer, positioned with the tip in the pulmonary artery, and secured for determination of pulmonary arterial pressure and thermal dilution cardiac output (CO), and was placed to facilitate right atrial administration of the ketamine and physiologic markers. The side arm of the sheath introducer was used for maintenance fluid administration and the readministration of autologous blood. Hydration was maintained throughout the study

by an infusion of 0.9% saline at a rate of 5–10 ml · kg^{-1} · h^{-1} to maintain a constant pulmonary artery diastolic pressure (± 2 mmHg).

After anesthetic induction and catheter placement, 150 ml whole blood was removed from the dog through the arterial catheter and anticoagulated with 1,000 U heparin. This blood was immediately replaced with 600 ml saline solution, 0.9%, administered intravenously over 30 min. During the first 10 min of the study (from time t = 0 min to t = 10 min), this autologous blood was reinfused intravenously to replace the blood removed during this period of frequent blood sampling.

The study was not begun until the dog was hemodynamically stable. This was defined as less than 10% variation of CO and pulmonary and systemic arterial blood pressures over a 30-min period when heart rate and blood pressures were measured continuously and CO was determined at least every 15 min. The dogs were hemodynamically stable approximately 1 h after removal and saline replacement of the 150 ml blood.

At the onset of the study (time t = 0 min), ICG (Hynson, Westcott, and Dunning, Baltimore, MD), 5 mg in 1 ml diluent, antipyrine (Sigma, St. Louis, MO), 25 mg in 1 ml of diluent, and racemic ketamine (Parke Davis, Morris Plains, NJ), 100 mg in 1 ml, were placed sequentially in a 76-cm intravenous tubing (4.25 ml priming volume). The 3-ml drug volume was flushed through the proximal pulmonary artery catheter port within 4 s using 10 ml dextrose in water, 5%, allowing the simultaneous determination of dye and thermal dilution CO. Arterial blood samples were collected every 0.05 min for the first min and every 0.1 min for the next minute using a computer-controlled roller pump (Cole-Parmer, Chicago, IL), set at a withdrawal rate of 1 ml/s, and a chromatography fraction collector (Model 203; Gilson, Middleton, WI). Subsequently, 30, 3-ml arterial blood samples were drawn manually at 0.5 min intervals to 4 min, at 5 and 6 min, every 2 min to 20 min, at 25 and 30 min, every 10 min to 60 min, every 15 min to 120 min, and every 30 min to 360 min.

Analytical Methods

Plasma ICG concentrations of all samples obtained up to 20 min were measured on the study day by the high-performance liquid chromatography (HPLC) technique of Grasela *et al.,*[18] as modified in our laboratory to provide sensitivity of 0.2–20.00 μg/ml with coefficients of variation of 5% or less.[19]

Plasma antipyrine concentrations were measured in all samples using a modification of a high-performance liquid chromatography technique developed in our laboratory.[10,20] The antipyrine method is linear for plasma concentrations of 0.10–10.00 μg/ml, with coefficients of variation of 5% or less.

Plasma [*S*-(−)] and [*R*-(+)] ketamine enantiomer concentrations were measured in all samples using a modification of the stereospecific high-performance liquid chromatography technique developed by Geisslinger *et al.*[21] Plasma samples were extracted in duplicate with C18 Empore high-performance extraction disk cartridges (3M Filtration Products, St. Paul, MN) using prilocaine as the internal standard. Samples were eluted isocratically at 1.0 ml/min from acid glycoprotein (AGP) guard and analytical columns (Advanced Separation Technologies, Inc., Whippany, NJ) using a mobile phase consisting of pH 6.98, 0.02 M phosphate buffer, and isopropyl alcohol in a 97.5:2.5 ratio. Absorbance was monitored at 214 nm. The stereoselective ketamine assay is linear from concentrations of 0.05 to 10.00 μg/ml, with coefficients of variation of 10% or less.

Plasma ICG concentrations were converted to blood concentrations by multiplying them by one minus the hematocrit because ICG does not partition into erythrocytes. To interpret intercompartmental clearances in relation to blood flow, plasma antipyrine and ketamine concentrations were corrected for partitioning into the erythrocyte by calculating the apparent dose of the respective drug. The ratio of the actual dose to the apparent or calculated dose is then used as an *in vivo* estimate of erythrocyte partitioning to convert plasma concentrations to blood concentrations. Because the central blood flow of the antipyrine and ketamine models was constrained to that of ICG (*i.e.,* CO), the apparent antipyrine and ketamine doses were estimated using blood ICG and plasma antipyrine or ketamine stereoisomer concentrations, respectively, obtained before the first evidence of recirculation according to the following relationship:[10]

$$\text{dose}_{\text{antipyrine or ketamine stereoisomer}} = \text{dose}_{\text{ICG}}/\text{AUC}_{\text{ICG}} \cdot \text{AUC}_{\text{antipyrine or ketamine stereoisomer}}$$

Data Analysis. A delay (central volume [V_C] and nondistributive volume [V_{ND}]; fig. 1) is a mathematical description of the distribution of drug transit times that can be described by the mean transit time (MTT). The apparent volume of a delay element can be determined as the product of the flow through the delay and its MTT. The delay elements of the SAAM II kinetics analysis software (SAAM Institute, Seattle, WA) are composed of a linear chain (or tanks-in-series) of n identical compart-

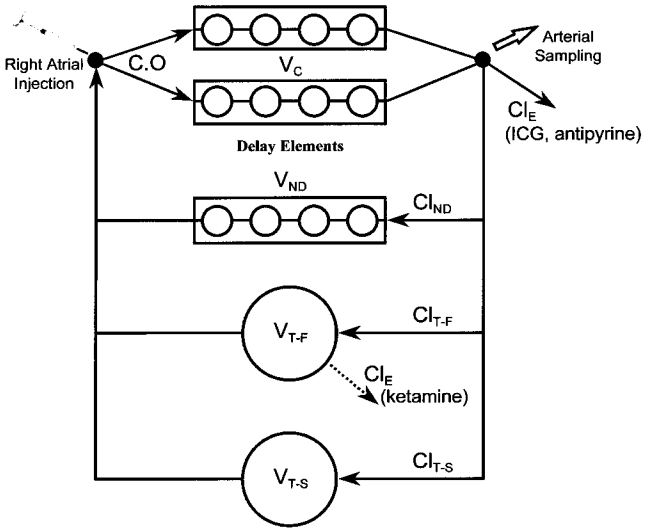

Fig. 1. The general model for the recirculatory pharmacokinetics of indocyanine green (ICG), antipyrine, and ketamine. The central circulation of all three drugs receives all of the cardiac output (CO) defined by the delay elements (V_C). The delay elements are represented generically by rectangles surrounding four compartments, although the actual number of compartments necessary varied between 2 and 30 for any particular delay. The pulmonary tissue volume (V_{T-P}), a subset of V_C, can be calculated for antipyrine and ketamine by subtracting the V_C of ICG from the V_C of antipyrine or ketamine, respectively. Beyond the central circulation, the CO distributes to numerous circulatory and tissue pathways that lump, on the basis of their blood volume to blood flow ratios or tissue volume to distribution clearance ratios (mean transit times), into fast (Cl_{ND-F}, V_{ND-F}) and slow (Cl_{ND-S}, V_{ND-S}) peripheral blood circuits (ICG) or nondistributive peripheral pathways (ketamine and antipyrine) and fast (Cl_{T-F}, V_{T-F}) and slow (Cl_{T-S}, V_{T-S}) tissue volume groups. ICG, which distributes only within the intravascular space, does not have fast and slow tissue volumes. The nondistributive flow for ICG was resolved into fast and slow components (not shown); antipyrine and ketamine do not have an identifiable second nondistributive peripheral circuit. The elimination clearance (Cl_E) of ICG and antipyrine are modeled from the arterial sampling site without being associated with any particular peripheral circuit, whereas the Cl_E of ketamine is modeled from V_{T-F} (model 4, see text).

ments connected by identical rate constants k such that n/k is equal to the MTT of the delay. The solution for a linear chain obtained by successive integration for the exit rate from compartment n is given by the Erlang density function, which is a special case of the τ distribution function,[22]

$$f(t) = (k^n \cdot t^{n-1}/(n-1)! \cdot e^{-kt}$$

Indocyanine green, antipyrine, and ketamine concentration *versus* time data before evidence of recirculation (*i.e.*, first-pass data) were weighted uniformly and fitted to the sum of two right-skewed τ (Erlang) distribution functions using TableCurve2D (version 3.0; Jandel Scientific, San Rafael, CA) on a desktop personal computer (Gateway 2000, North Sioux City, SD).[22] The application of classic criteria for defining first-pass concentration to our data analysis using the Erlang distribution function has been described in detail by Krejcie *et al.*[22] Because paired first-pass *S*-(+)- and *R*-(−)-ketamine concentrations and the respective pulmonary MTT for the enantiomers were not different (paired *t* test), *S*-(+)- and *R*-(−)-ketamine concentrations were modeled simultaneously; this improved the confidence in the model parameters of ketamine pulmonary uptake. Erlang functions were not used to determine V_{ND}, instead single delay elements in SAAM II were used in which the optimum number of tanks-in-series were determined iteratively.

In subsequent pharmacokinetic analysis, the descriptions of the central circulation (the blood and apparent tissue volume between the right atrial injection site and the femoral arterial sampling site) were incorporated as parallel linear chains, or delay elements, into independent recirculatory models for the individual markers using SAAM II implemented on a desktop personal computer (Gateway 2000).[9,22] The first-pass data were excluded from further data fitting; the results of the Erlang model of the central circulation were placed as fixed parameters in the recirculatory model, thereby reducing the number of parameters to be optimized. The concentration–time data were weighted, assuming a proportional variance model, in proportion to the inverse of the square of the predicted value. Possible systematic deviations of the observed data from the calculated values were sought[23] using the two-tailed one-sample runs test, with $P < 0.05$ corrected for multiple applications of the runs test, as the criterion for rejection of the null hypothesis.[24] Possible model misspecification was sought by evaluating the ratio of the measured to the predicted drug concentrations *versus* time relation.

The Pharmacokinetic Model

The pharmacokinetic modeling methodology has been previously described in detail.[11] It is based on the approach described by Jacquez[25] for obtaining information from outflow concentration histories, the so-called inverse problem. Antipyrine and ketamine distributions were analyzed as the convolution of their intravascular behavior, determined by the pharmacokinetics of concomitantly administered ICG, and tissue distribution kinetics.[10]

For ICG, the two lumped, parallel pathways of the central circulation, described by the sum of two Erlang

distribution functions, were incorporated in a full recirculatory model (fig. 1), including lumped parallel fast and slow peripheral intravascular circuits and Cl_E using SAAM II. The antipyrine and ketamine pulmonary tissue volumes ($V_{T\text{-}P}$) are the difference between their respective apparent central volumes ($MTT_{antipyrine\ or\ ketamine} \cdot CO$) and the central intravascular volume determined by ICG ($MTT_{ICG} \cdot CO$).

Peripheral drug distribution can be lumped into identifiable volumes and clearances: a fast nondistributive peripheral pathway ($V_{ND\text{-}F}$ and $Cl_{ND\text{-}F}$); a slow nondistributive peripheral pathway ($V_{ND\text{-}S}$ and $Cl_{ND\text{-}S}$); rapidly (fast) equilibrating tissues ($V_{T\text{-}F}$ and $Cl_{T\text{-}F}$); and slowly equilibrating tissues ($V_{T\text{-}S}$ and $Cl_{T\text{-}S}$). The nondistributive peripheral pathways (delay elements) represent intravascular circuits in the ICG model.[10,19] The single nondistributive peripheral pathway in the antipyrine and ketamine models, determined by the respective recirculation peaks, represents blood flow that quickly returns the lipophilic drugs to the central circulation after minimal tissue distribution (*i.e.,* a pharmacokinetic shunt).[10,11] In the antipyrine and ketamine models, the parallel rapidly and slowly equilibrating tissues are the fast and slow compartments of traditional three-compartment pharmacokinetic models; therefore, the central circulation and nondistributive peripheral pathways are detailed representations of the ideal central volume of the three-compartment model.[20] Because of the direct correspondence between the recirculatory model and three-compartment models, Cl_E was modeled from the arterial (sampling) compartment to enable comparison of these results with previous ones.

As noted previously, preliminary analyses of the first-pass *S*-(+)- and *R*-(−)-ketamine arterial plasma concentration data indicated that there were no differences in pulmonary tissue distribution for these enantiomers, suggesting that their distribution to other tissues may also be indistinguishable from one another; *i.e.,* intercompartmental clearances and volumes of distribution are the same for each enantiomer. To test this hypothesis, ketamine data were fit to models in which the number of parameters describing peripheral drug distribution were successively decreased. To determine statistically which was the simplest model, the Akaike information criterion (AIC),[29] the mean absolute performance error (MAPE) and visual inspection of the plots of the ratios of the measured to the predicted drug concentrations *versus* time relations were used as bases for model selection.

$$MAPE = \frac{1}{n}\sum_{i=1}^{n} APE_i$$

$$APE = |C_{pred} - C_{meas}/C_{pred}| \cdot 100$$

For model 1, Cl_E, intercompartmental clearances (Cl_{ND}, $Cl_{T\text{-}F}$, and $Cl_{T\text{-}S}$), and distribution volumes (V_{ND}, $V_{T\text{-}F}$, and $V_{T\text{-}S}$) for the two enantiomers were independent of one another (12 parameters). For model 2, Cl_E and the distribution volumes remained independent, but all of the intercompartmental clearances were the same for the enantiomers, except Cl_{ND}, which was allowed to vary reciprocally with the different Cl_Es because both of these clearances are nondistributive and their sum was assumed to be the same for both enantiomers (10 parameters). For model 3, Cl_E, Cl_{ND}, and V_{ND} were allowed to vary, but tissue volumes and their respective intercompartmental clearances were set to be equal (eight parameters).

Other investigators reported differences in the tissue distribution models for ketamine enantiomers.[4,5] The apparent differences in tissue distribution of the ketamine enantiomers may be derived from an artifact of modeling the different Cl_Es of the stereoisomers from V_C. Modeling Cl_E from a peripheral compartment rather than V_C will affect the estimate of the volume of the peripheral compartment from which Cl_E is modeled, and thus the steady state volume of distribution (V_{SS}).[26] Normally, there is no information in typical input–output pharmacokinetic data to select among elimination models,[27] but the simultaneous modeling of enantiomers with different Cl_Es and similar tissue distribution should enable optimal model selection. Therefore, a fourth model was considered (model 4), with elimination modeled from $V_{T\text{-}F}$ instead of V_C and only Cl_E was allowed to vary for the two enantiomers (six parameters). $V_{T\text{-}F}$ was chosen because this compartment includes the major portion of the splanchnic circulation and tissue.[10,28]

Results

Blood ICG, antipyrine, and ketamine enantiomer concentration *versus* time relations were well-characterized by the models from the moment of drug administration (time t = 0; figs. 2–4). The arterial blood drug concentration *versus* time relations were always characterized by a brief delay between the moment of drug administration and their appearance at the arterial blood sampling site. The one-sample runs test indicated that there

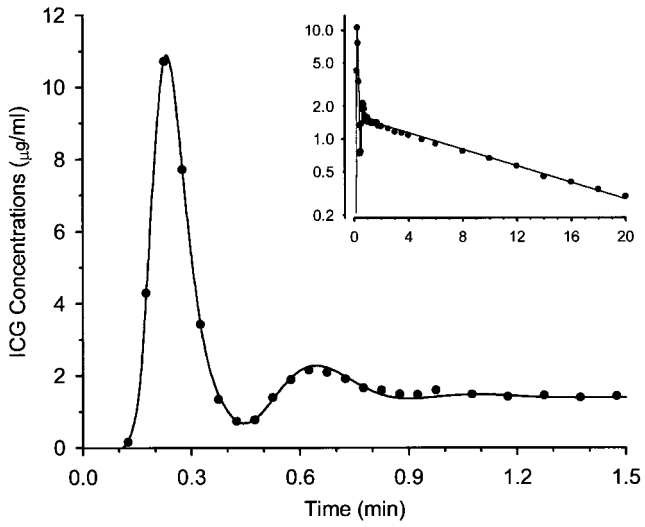

Fig. 2. Arterial blood indocyanine green (ICG) concentration histories for the first 1.5 min (illustrating the first- and second-pass peaks) and for 20 min (*inset*) after right atrial injection in dog 1. The symbols represent drug concentrations, whereas the lines represent concentrations predicted by the model.

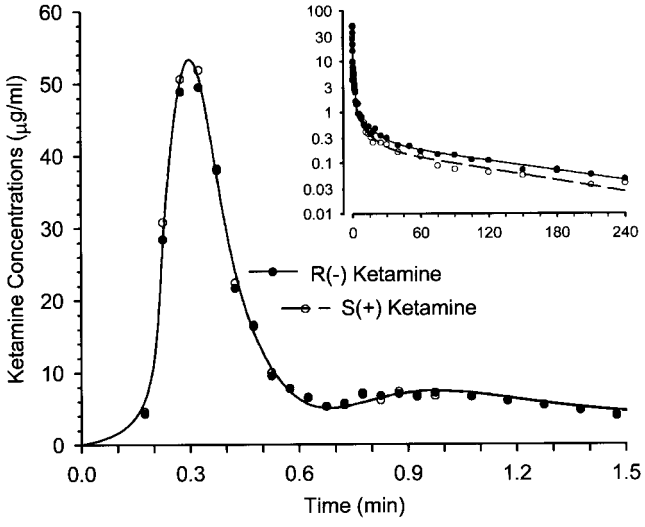

Fig. 4. Arterial blood *S*-(+)-ketamine (open symbols) and *R*-(−)-ketamine (closed symbols) concentration histories for the first 1.5 min (illustrating the first- and second-pass peaks) and for 240 min (*inset*) after right atrial injection in dog 1. The symbols represent drug concentrations, whereas the lines represent concentrations predicted by the models. Note that several open symbols are obscured by being coincident with closed symbols.

were no systematic deviations of the observed data from the calculated values.

The recirculatory pharmacokinetic model parameters of ICG are presented in table 2. A little more than one third of the blood volume (0.95 of 2.68 l) was in the central circuits. The fast peripheral circuit contained 0.20 l, which is an average of 11.7% of the peripheral blood volume (1.73 l) and 7.7% of the total blood volume, and received 48.3% (1.77 l/min) of CO (3.58 l/min, as determined by dye dilution, table 2). The slow circuit contained the majority of the peripheral blood volume (88.3%, 1.53 l, which is 56.9% of the total blood volume) but received only 41.9% (1.49 l/min) of CO ICG Cl_E represented only 9.9% (0.30 l/min) of CO.

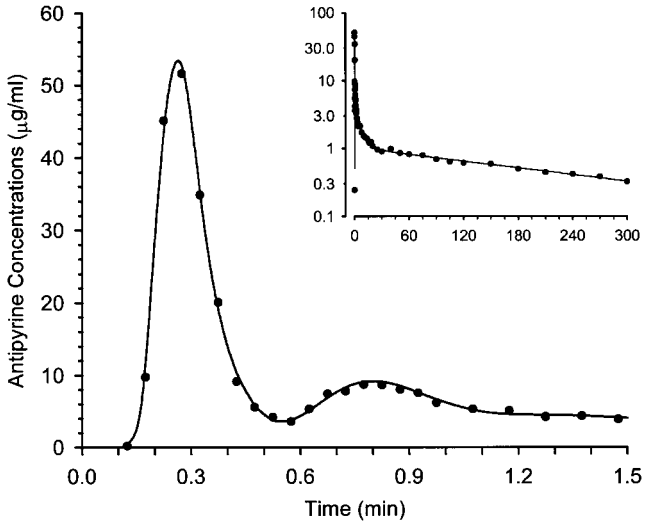

Fig. 3. Arterial blood antipyrine concentration histories for the first 1.5 min (illustrating the first- and second-pass peaks) and for 300 min (*inset*) after right atrial injection in dog 1. The symbols represent drug concentrations, whereas the lines represent concentrations predicted by the models.

The recirculatory antipyrine pharmacokinetic model (table 2) always contained a small but readily identifiable pulmonary tissue volume, which averaged 0.16 l or 0.61% of the total antipyrine distribution volume (26.6 l). The rapidly and slowly equilibrating peripheral antipyrine tissue volumes contained an average of 19.0% (5.02 l) and 75.5% (20.09 l) of the total antipyrine distribution volume, respectively, and fast and slow distribution clearances averaged 44.0% (1.64 l/min) and 21.5% (0.82 l/min) of CO, respectively. Antipyrine Cl_E accounted for only 2.9% (0.10 l/min) of CO. The balance of CO in the antipyrine model (31.5%, 1.02 l/min) was assigned to the nondistributive peripheral pathway, which represented only 1.3% (0.33 l) of the total antipyrine distribution volume.

The AIC for the various recirculatory ketamine pharmacokinetic models in table 3 shows that there was an improvement in AIC (lowering) from model 1 to model 2 in which the number of independent param-

Table 2. Pharmacokinetic Variables for Recirculatory Indocyanine Green (ICG), Antipyrine, and Ketamine Pharmacokinetics [Mean (SD)] (N = 5)

	Volumes (l)*							Clearances (l/min)†							
Marker	V_C	V_{T-P}	V_{ND-F}	V_{ND-S}	V_{T-F}	V_{T-S}	V_{SS}	Cl_{ND-F}	Cl_{ND-S}	Cl_{T-F}	Cl_{T-S}	Cl_E	$S(+)$ Cl_E	$R(-)$ Cl_E	ΣCl
ICG	0.95 (0.21)		0.20 (0.11)	1.53 (0.24)			2.68 (0.21)	1.77 (1.18)	1.49 (0.73)			0.30 (0.08)			3.58 (1.59)
Antipyrine	1.11 (0.29)	0.16 (0.08)	0.33 (0.10)		5.02 (1.29)	20.1 (3.54)	26.6 (3.84)	1.02 (0.27)		1.64 (0.89)	0.82 (0.50)	0.10 (0.03)			3.58 (1.59)
Ketamine (model 4)	1.26 (0.28)	0.31 (0.09)	0.48 (0.44)		6.17 (3.40)	38.5 (14.0)	46.4 (14.9)	1.17 (0.53)		1.54 (0.66)	0.86 (0.68)		0.66 (0.13)	0.49 (0.09)	3.58 (1.59)

* The volumes (V) of the two parallel central (C) circuits [including the pulmonary tissue (T-P)], the rapidly equilibrating (fast) nondistributive (ND-F) and slowly equilibrating nondistributive (ND-S) circuits, and the rapidly equilibrating (fast) (T-F) and slowly equilibrating (T-S) tissues. The volume of distribution at steady-state (V_{SS}) equals the sum of all volumes except the antipyrine and ketamine pulmonary volumes, which are represented in their V_Cs because antipyrine and ketamine V_{T-P} are equal to the difference between the antipyrine and ketamine V_Cs and the V_C described by ICG, respectively.

† The clearances (Cl) of the rapidly (fast) equilibrating nondistributive (ND-F) and slowly equilibrating nondistributive (ND-S) intravascular circuits, and the rapidly equilibrating (fast) (T-F) and slowly equilibrating (T-S) tissues, elimination clearance (Cl_E), and the sum of all clearances (ΣCl), which equals the ICG (dye dilution) cardiac output determined at the moment of marker injection. ΣCl in the ketamine peripheral elimination model includes only the sum of intercompartmental clearances because Cl_E in this model is already represented in the clearance (Cl_{T-F}) to the compartment from which Cl_E is modeled (V_{T-F}).

eters was reduced by two by setting the intercompartmental clearances of the racemates to be equal. However, the AIC increased in model 3, in which there was a further reduction in the number of parameters by setting the peripheral tissue volumes to be equal. Therefore, we rejected the model in which the ketamine racemates distributed to similar tissue volumes when elimination was modeled from the central compartment. However, the lowest (*i.e.*, most negative) AIC in all dogs was observed in a peripheral elimination model: model 4. The reduction in the number of adjustable parameters afforded by this model (six fewer than model 1, four fewer than model 2, and two fewer than model 3) did not result in a marked increase in mean absolute performance error over that of the models (1, 2, and 3) with more adjustable parameters. Only the central elimination model with the largest number of degrees of freedom, model 1 with independent intercompartmental clearances and peripheral volumes, had slightly better mean absolute performance errors than model 4 for most dogs. Therefore, the ketamine pharmacokinetic results reported and discussed herein are those of model 4.

The recirculatory ketamine pharmacokinetic model (table 2) also contained a pulmonary tissue volume, which averaged 0.31 l and was 0.75% of the total ketamine distribution volume (46.4 l). The rapidly (6.17 l) and slowly (38.48 l) equilibrating peripheral ketamine tissue volumes contained an average of 13.9 and 82.0% of the total ketamine distribution volume (46.4 l), respectively. Fast (1.54 l/min) and slow (0.86 l/min) distribution clearances averaged 44.3 and 21.9% of CO, respectively. Ketamine Cl_E was greater for the *S*-(+)-enantiomer (0.66 l/min) than for the *R*-(−)-enantiomer

Table 3. Measures of Model Selection (AIC*) and Goodness of Fit (MAPE) for Models of Ketamine Stereoisomer Disposition with Central Elimination or Elimination Modeled from a Peripheral Compartment (V_{T-F})† (N = 5)

	AIC				MAPE			
	Central Elimination			Peripheral Elimination (Model 4)	Central Elimination			Peripheral (Model 4)
Elimination	Model 1	Model 2	Model 3		Model 1	Model 2	Model 3	
Mean	−0.77	−0.80	−0.73	−0.82	7.06	7.61	7.86	7.14

* A lower (*i.e.,* more negative) score connotes a more statistically justified model.

† Model 1: Distribution volumes, intercompartmental, and elimination clearances of the two enantiomers were modeled independently. Model 2: Intercompartmental clearances (except Cl_{ND}) of the two enantiomers were the same; distribution volumes, Cl_E, and Cl_{ND} were modeled independently for each enantiomer. Model 3: Distribution volumes and intercompartmental clearances (except Cl_{ND}) of the two enantiomers were the same; Cl_E and Cl_{ND} were modeled independently for each enantiomer. Model 4: Distribution volumes and intercompartmental clearances of the two enantiomers were the same; Cl_E was modeled from V_{T-F} independently for each enantiomer.

(0.49 l/min). The intercompartmental clearance to the nondistributive peripheral pathway (1.17 l/min) was 33.9% of CO, whereas the nondistributive volume (0.48 l) represented only 1.0% of the total ketamine distribution volume.

Discussion

The intensity and timing of the onset of drug effect for rapidly acting intravenous anesthetics, such a ketamine, are influenced by factors affecting the early arterial drug concentration *versus* time profile.[8] These factors include intravascular mixing, pulmonary uptake, and distribution to highly perfused tissues.[9,30] It has been suggested recently that distribution of drugs to tissue may be affected more by active transport across the endothelium than by factors such as blood flow and diffusion.[12] Recently, we showed that the pulmonary uptake of fentanyl involves, not only passive diffusion, but also carrier-mediated endothelial transport.[13] Ketamine is a racemic (50:50) mixture of two enantiomers that have been shown to interact with proteins in a stereospecific fashion. The *S*-(+)-enantiomer binds to NMDA receptors more avidly than the does the *R*-(−)-enantiomer,[31] producing a more potent hypnotic effect.[6] Likewise, human hepatic microsomes *N*-demethylate the *S*-(+)-enantiomer at a higher rate than *R*-(−)-ketamine.[32] We wished to measure the *in vivo* tissue distribution of ketamine and to determine whether there may be differences in the distribution of the stereoisomers, which would be suggestive of a specific protein-mediated transport across the vascular endothelium. In addition, we wished to evaluate ketamine pharmacokinetics using a high-resolution recirculatory model to examine carefully any possible differences in disposition that could reasonably be attributed to differential handling of the two stereoisomers.

The estimate of pulmonary extravascular antipyrine distribution ($V_{T\text{-}P}$, 0.16 ± 0.08 l) corresponds well with estimates of others for pulmonary extravascular water volume in dogs.[33] Ketamine $V_{T\text{-}P}$ was twice that of antipyrine (table 2). There was no difference in the $V_{T\text{-}P}$ of the *R*-(−)- and *S*-(+)-ketamine enantiomers. We looked for systematic differences between stereoisomer concentrations in each sample collected during first-pass and found none. In addition, there was no difference in the first-pass MTT, the principal measure of pulmonary uptake.[22,30,34] The lack of a stereoisomeric effect in the pulmonary tissue distribution of ketamine suggests that physicochemical differences other than stereoisomerism account for its increased partitioning in the lung compared with antipyrine.

The pulmonary uptake of ketamine is quite small compared with fentanyl (60 times tissue water),[13] lidocaine (9 times tissue water)[9] or sufentanil (84 times tissue water).[30] It is closer to that of alfentanil (2.4 times tissue water)[22,34] or diazepam (approximately 5 times tissue water).[34] Thus, interindividual differences in the pulmonary uptake of ketamine would not be expected to have much of an effect on onset of action.

The lack of stereoisomeric effect for the distribution of ketamine in pulmonary tissue suggests that the distribution of the *S*-(+) and *R*-(−)-enantiomers in other tissues might also be identical. Because the pharmacokinetics of tissue distribution are described by intercompartmental clearance ($Cl_{T\text{-}F}$ and $Cl_{T\text{-}S}$) and volume of distribution ($V_{T\text{-}F}$ and $V_{T\text{-}S}$), we systematically explored the modeling implications (*i.e.*, goodness of fit *vs.* number of adjustable parameters) of treating the enantiomers as individual drugs or as identical drugs with respect to these parameters. If these parameters can be made to be common to the two enantiomers without substantially affecting goodness of fit, the AIC should become progressively smaller as more distribution parameters are made common. Table 3 shows that in the case of a central elimination model this is true if $Cl_{T\text{-}F}$ and $Cl_{T\text{-}S}$ are made common, but does not hold up if $V_{T\text{-}F}$ and $V_{T\text{-}S}$ are also made common. Because the *S*-(+)-enantiomer has the greater Cl_E, we would expect its peripheral distribution volume to be less than that of the *R*-(−)-enantiomer during this condition. With Cl_E modeled from $V_{T\text{-}F}$, we obtained similar fits with fewer adjustable parameters and an improved AIC (fig. 5 and table 3); that is, there was a consistent improvement in the AIC when both enantiomers were "forced" to share the same $V_{T\text{-}F}$, $V_{T\text{-}S}$, $Cl_{T\text{-}F}$, and $Cl_{T\text{-}S}$. Thus, it is reasonable to conclude that there are no significant differences in the pharmacokinetics of tissue distribution between the two enantiomers of ketamine. This exercise provides evidence that the choice of the site from which Cl_E is modeled (*i.e.,* central or peripheral) will affect the peripheral distribution volume and thus V_{SS}.

Using a central elimination model with all parameters independent for the two enantiomers (model 1) resulted in a V_{SS} for *R*-(−)-ketamine of 55.8 l, compared with 42.9 l for *S*-(+)-ketamine. This is in contrast to the peripheral elimination model (model 4) in which the V_{SS} for either enantiomer was 46.4 l. Using model 1, the Cl_Es were 0.49 and 0.66 l/min, respectively, the same as

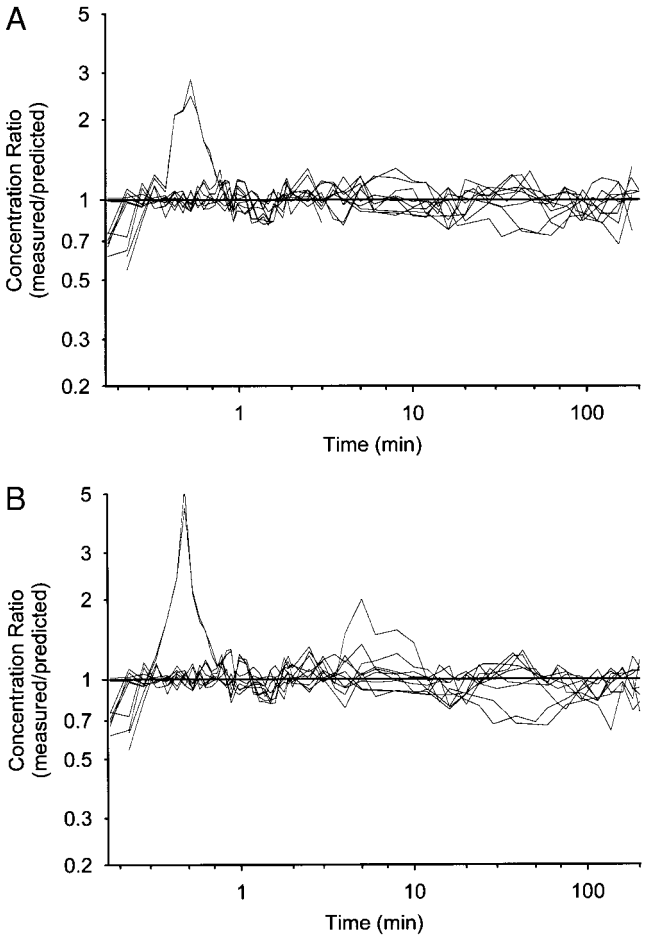

Fig. 5. (*A*) Graphs of the ratio of measured to predicted drug concentrations *versus* time relations for *S*-(+)- and *R*-(−)-ketamine in all five dogs. Predicted concentrations are from the ketamine models in which Cl_E is modeled from the arterial sampling site (central) and all distribution parameters are adjusted independently (model 1). (*B*) Graphs of the ratio of measured to predicted drug concentrations *versus* time relations for *S*-(+)- and *R*-(−)-ketamine in all five dogs. Predicted concentrations are from the ketamine models in which Cl_E is modeled from the rapidly equilibrating peripheral tissue compartment (peripheral) and all distribution parameters are adjusted such that they are the same for the *S*-(+)- and *R*-(−)-enantiomers (model 4).

reported for model 4 in table 2 because elimination clearance is independent of the model used.

The ketamine V_{SS} (model 4) in these five dogs averaged 2.11 l/kg when referenced to plasma and compared with 2.5 l/kg reported by Kaka and Hayton[35] and with 1.37 l/kg reported by Schwieger *et al.*[36] The total (*i.e.,* racemic) ketamine Cl_E values reported in these studies were 32.2 and 18.1 ml · min^{-1} · kg^{-1}, respectively, compared with 22.2 ml · min^{-1} · kg^{-1} for *R*-(−)-ketamine and 29.9 ml · min^{-1} · kg^{-1} for *S*-(+)-ketamine (table 1) in the current study.

There was a marked difference in Cl_E for the two enantiomers of ketamine. On average, the Cl_E was 35% greater for the *S*-(+)-enantiomer compared with the *R*-(−)-enantiomer and was greater in all five dogs (table 2). This is consistent with the results of White *et al.*[3] and Geisslinger *et al.*[4,5] in humans (15 and 22% greater, respectively) and previous findings in rodents.[1,2] In human liver microsomes, Kharasch and Labroo[32] showed that the rate of *N*-demethylation was greater for *S*-(+)-ketamine than for the *R*-(−)-enantiomer.

The ICG and antipyrine kinetics compare very well with those from previous studies during similar conditions,[9–11,19,20,22] suggesting that the 100-mg dose of ketamine had little if any effect on the factors governing the pharmacokinetics of these markers and drugs. Only in dog 2 was there a brief period of systematically poor fitting. This incident corresponds to the large positive deflection just before 1 min in the measure to predicted drug concentration ratio *versus* time plots (fig. 5). This may be the result of a brief hemodynamic perturbation in this dog caused by the ketamine bolus. Because of the need for near-continuous arterial sampling, no hemodynamic measurements could be made during this period. However, at t = 10 min, all such values were within 10% of baseline.

Although antipyrine and ketamine were modeled independently, their mean intercompartmental clearances ($Cl_{T\text{-}F}$ and $Cl_{T\text{-}S}$) and the nondistributive intercompartmental clearances (Cl_{ND}) were remarkably similar. A linear regression for these parameters is shown in figure 6 and shows that the correlations were highly significant for $Cl_{T\text{-}F}$ and $Cl_{T\text{-}S}$; the correlation for Cl_{ND} was not significant because of an outlying datum. This finding suggests that a further model-reduction step, whereby the enantiomers of ketamine share common distribution clearance terms with antipyrine, could be made. It also indicates that factors determining the transcapillary exchange of these two compounds are similar. Antipyrine has been used as a marker of perfusion-limited tissue distribution in many tissues[17] because it is minimally plasma protein bound, freely diffuses across lipid membranes, and equilibrates very rapidly with tissues. It would appear that the transcapillary exchange of ketamine is similar to that of antipyrine, despite ketamine's more extensive plasma protein binding (53%),[35] indicating that the protein binding of ketamine does not influence its transcapillary exchange.

We described the pulmonary uptake and recirculatory

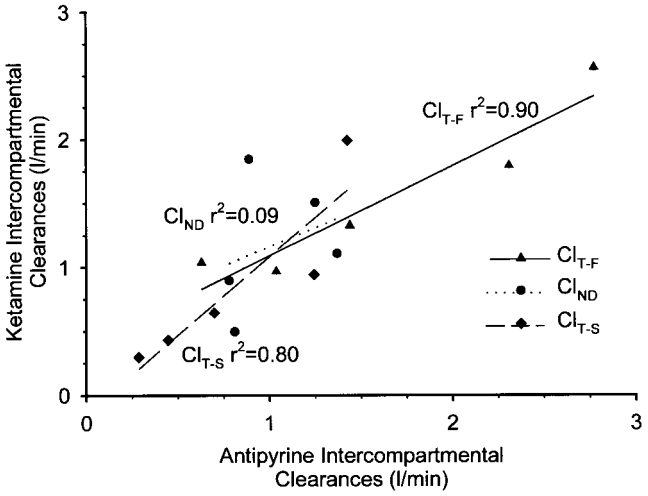

Fig. 6. Linear regressions of antipyrine clearances Cl_{ND}, Cl_{T-F}, and Cl_{T-S} *versus* the individual corresponding ketamine clearances in the five dogs. The squared value of the correlation coefficient for each regression is displayed on the graph. The ketamine intercompartmental clearance axis intercept (approximately 0.39 l/min) for the Cl_{T-F} regression probably reflects the inclusion of Cl_E in the estimates of these parameters for ketamine but not for antipyrine, as a result of modeling elimination from the peripheral and central compartments, respectively.

pharmacokinetics of the individual stereoisomers of ketamine based on a multiple-indicator dilution technique with frequent arterial blood sample collection. Although the *S*-(+)-ketamine enantiomer had a Cl_E that averaged 35% more than the *R*-(−)-enantiomer, we found no difference in the pulmonary uptake of these two stereoisomers. Our conclusion that the peripheral distribution kinetics of the ketamine stereoisomers do not differ is predicated on the assumption that, if the pulmonary uptake of ketamine is not stereospecific, peripheral tissue distribution is unlikely to be stereospecific. Modeling the two different stereoisomer Cl_Es from V_{T-F} rather than from V_C yielded a model of ketamine stereoisomer tissue distribution that was consistent with this assumption.

References

1. Ryder S, Way WL, Trevor AJ: Comparative pharmacology of the optical isomers of ketamine in mice. Eur J Pharmacol 1978; 49:15–23

2. Marietta MP, Way WL, Castagnoli N Jr, Trevor AJ: On the pharmacology of the ketamine enantiomorphs in the rat. J Pharmacol Exp Ther 1977; 202:157–65

3. White PF, Schuttler J, Shafer A, Stanski DR, Horai Y, Trevor AJ: Comparative pharmacology of the ketamine isomers. Studies in volunteers. Br J Anaesth 1985; 57:197–203

4. Geisslinger G, Hering W, Thomann P, Knoll R, Kamp HD, Brune K: Pharmacokinetics and pharmacodynamics of ketamine enantiomers in surgical patients using a stereoselective analytical method. Br J Anaesth 1993; 70:666–71

5. Geisslinger G, Hering W, Kamp HD, Vollmers KO: Pharmacokinetics of ketamine enantiomers (letter). Br J Anaesth 1995; 75:506–7

6. Schuttler J, Stanski DR, White PF, Trevor AJ, Horai Y, Verotta D, Sheiner LB: Pharmacodynamic modeling of the EEG effects of ketamine and its enantiomers in man. J Pharmacokinet Biopharm 1987; 15: 241–53

7. Schuttler J: *S*-(+)-ketamine. The beginning of a new ketamine era? (editorial; comment). Anaesthesist 1992; 41:585–7

8. Sheiner LB, Benet LZ, Pagliaro LA: A standard approach to compiling clinical pharmacokinetic data. J Pharmacokinet Biopharm 1981; 9:59–127

9. Krejcie TC, Avram MJ, Gentry WB, Niemann CU, Janowski MP, Henthorn TK: A recirculatory model of the pulmonary uptake and pharmacokinetics of lidocaine based on analysis of arterial and mixed venous data from dogs. J Pharmacokinet Biopharm 1997; 25:169–90

10. Krejcie TC, Henthorn TK, Niemann CU, Klein C, Gupta DK, Gentry WB, Shanks CA, Avram MJ: Recirculatory pharmacokinetic models of markers of blood, extracellular fluid and total body water administered concomitantly. J Pharmacol Exp Ther 1996; 278: 1050–7

11. Avram MJ, Krejcie TC, Niemann CU, Klein C, Gentry WB, Shanks CA, Henthorn TK: The effect of halothane on the recirculatory pharmacokinetics of physiologic markers. ANESTHESIOLOGY 1997; 87:1381–93

12. Wood M: Drug distribution: Less passive, more active (editorial)? ANESTHESIOLOGY 1997; 87:1274–6

13. Waters CM, Avram MJ, Krejcie TC, Henthorn TK: Uptake of fentanyl in pulmonary endothelium. J Phamacol Exp Ther 1999;288: 157–63

14. Renkin EM: Capillary permeability to lipid soluble molecules. Am J Physiol 1952; 168:538–45

15. Soberman R, Brodie BB, Levy BB, Axelrod J, Hollander V, Steele JM: The use of antipyrine in the measurement of total body water in man. J Biol Chem 1949;179:31–42

16. Brigham KL, Ramsey LH, Snell JD, Merritt CR: On defining the pulmonary extravascular water volume. Circ Res 1971; 29:385–97

17. Renkin EM: Effects of blood flow on diffusion kinetics in isolated perfused hindlegs of cats. Am J Physiol 1955; 183:125–36

18. Grasela DM, Rocci ML Jr, Vlasses PH: Experimental impact of assay-dependent differences in plasma indocyanine green concentration determinations. J Pharmacokinet Biopharm 1987;15: 601–13

19. Henthorn TK, Avram MJ, Krejcie TC, Shanks CA, Asada A, Kaczynski DA: Minimal compartmental model of circulatory mixing of indocyanine green. Am J Physiol 1992; 262:H903–10

20. Krejcie TC, Henthorn TK, Shanks CA, Avram MJ: A recirculatory pharmacokinetic model describing the circulatory mixing, tissue distribution and elimination of antipyrine in dogs. J Pharmacol Exp Ther 1994; 269:609–16

21. Geisslinger G, Menzel-Soglowek S, Kamp H-D, Brune K: Stereoselective high-performance liquid chromatographic determination of the enantiomers of ketamine and norketamine in plasma. J Chromatogr 1991; 568:165–76

22. Krejcie TC, Jacquez JA, Avram MJ, Niemann CU, Shanks CA,

Henthorn TK: Use of parallel Erlang density functions to analyze first-pass pulmonary uptake of multiple indicators in dogs. J Pharmacokinet Biopharm 1996; 24:569–88

23. Berman BS, Shahn E, Weiss MJ: The routine fitting of kinetic data to models: A mathematical formalism for digital computers. Biophys J 1962; 2:275–87

24. Siegel S: Nonparametric Statistics for the Behavioral Sciences. New York, McGraw-Hill, 1956

25. Jacquez JA: Compartmental Analysis in Biology and Medicine, 3rd edition. Ann Arbor, BioMedware, 1996

26. Henthorn TK, Avram MJ, Krejcie TC: Intravascular mixing and drug distribution: The concurrent disposition of thiopental and indocyanine green. Clin Pharmacol Ther 1989; 45:56–65

27. Godfrey KR, Chapman MJ, Vajda S: Identifiability and indistinguishability of nonlinear pharmacokinetic models. J Pharmacokinet Biopharm 1994; 22:229–51

28. Sedek GS, Ruo IT, Frederiksen MC, Frederiksen JW, Shih SR, Atkinson AJ Jr: Splanchnic tissues are a major part of the rapid distribution spaces of inulin, urea and theophylline. J Pharmacol Exp Ther 1989; 251:1026–31

29. Ludden TM, Beal SL, Sheiner LB: Comparison of the Akaike information criterion, the Schwarz criterion and the F test as guides to model selection. J Pharmacokinet Biopharm 1994; 22:431–45

30. Boer F, Hoeft A, Scholz M, Bovill JG, Burm AG, Hak A: Pulmonary distribution of alfentanil and sufentanil studied with system dynamics analysis. J Pharmacokinet Biopharm 1996; 24:197–218

31. Lodge D, Anis NA, Burton NR: Effects of optical isomers of ketamine on excitation of cat and rat spinal neurones by amino acids and acetylcholine. Neurosci Lett 1982; 29:281–6

32. Kharasch ED, Labroo R: Metabolism of ketamine stereoisomers by human liver microsomes. ANESTHESIOLOGY 1992; 77:1201–7

33. Dawson CA, Christensen CW, Rickaby DA, Linehan JH, Johnston MR: Lung damage and pulmonary uptake of serotonin in intact dogs. J Appl Physiol 1985; 58:1761–6

34. Audi SH, Linehan JH, Krenz GS, Dawson CA, Ahlf SB, Roerig DL: Estimation of the pulmonary capillary transport function in isolated rabbit lungs. J Appl Physiol 1995; 78:1004–14

35. Kaka JS, Hayton WL: Pharmacokinetics of ketamine and two metabolites in the dog. J Pharmacokinet Biopharm 1980; 8:193–202

36. Schwieger IM, Szlam F, Hug CC Jr: The pharmacokinetics and pharmacodynamics of ketamine in dogs anesthetized with enflurane. J Pharmacokinet Biopharm 1991; 19:145–56